

Envelope Structure of Human eNOS Protein Revealed by Small-Angle X-ray Scattering

Chun-Yu Chen,¹ Pei-Feng Chen,² Yeukuang Hwu,³
U-Ser Jeng,¹ Kun-Yu Wu,² and Keng S. Liang^{1,4,*}

¹National Synchrotron Radiation Research Center, Hsinchu, Taiwan

²National Health Research Institutes, Zhunan Miaoli, Taiwan

³Institute of Physics, Academia Sinica, Taipei, Taiwan

⁴Department of Electrophysics, National Chiao Tung University, Hsinchu, Taiwan

(Received August 8, 2011)

We investigate the solution structure of human eNOS protein by using synchrotron small-angle X-ray scattering (SAXS). The pair-correlation analysis of the profile shows the radius of gyration (R_g) and maxima dimension (D_{\max}) of 6.87 ± 0.03 nm and 22 nm, respectively. The ratio of D_{\max} and R_g revealed that the protein was an extended conformation. The *ab initio* shape determination and rigid-body calculations were performed to reconstruct the real-space structure of eNOS in solution. The result shows that human eNOS form homodimer form in solution with the closed contact of two oxygenase domains.

PACS numbers: 61.05.cm, 68.18.-g, 61.25.H-

I. INTRODUCTION

Nitric oxide synthases (NOS) produce nitric oxide (NO), which participates in a variety of physiological processes such as neurotransmission, cardiovascular homeostasis, and immune modulation. Like that of the neuronal NOS (nNOS) and the inducible NOS (iNOS), the endothelial isoform (eNOS) consists of C-terminal reductase domain and N-terminal oxygenase domain. A calmodulin (CaM) binding peptide (residues 493–510) separates the oxygenase and reductase regions. It is generally believed that binding of CaM/Ca²⁺ to this canonical CaM-binding site enables a conformational change that facilitates electron transfer from the reductase domain to the oxygenase domain. Our recent work has demonstrated that two other regions, the proximal heme-binding site (residues 174–193) and the CD1 linker connecting FAD/FMN subdomains (residues 729–757), are possibly involved in CaM/Ca²⁺-regulated eNOS catalysis. The mechanics of calmodulin-dependent activation are complicated than we thought previously.

At present, *the three-dimensional structures of whole molecule of NOSs are lacking*. In this work, we investigate the molecular structure of human eNOS protein by using small-angle X-ray scattering (SAXS). The human eNOS solutions were prepared in the buffer containing 25 mM Tris-HCl, 100 mM NaCl, 2mM EGTA, and 10% glycerol. The SAXS experiments were performed at beamline BL23A with 14 keV X-ray beam at NSRRC.

*Electronic address: ksliang@nctu.edu.tw

The scattering profile was obtained for a q -range from 0.007 \AA^{-1} to 0.3 \AA^{-1} . The pair-correlation analysis of the profile shows the radius of gyration (R_g) and maxima dimension of $6.87 \pm 0.03 \text{ nm}$ and 22 nm , respectively. The envelope calculation was also performed by *ab initio* shape determination. The calculated scattering profile has a good fit to the measured profile of human eNOS protein. Interestingly, the envelope structure of human eNOS protein as revealed shows an extended conformation.

II. EXPERIMENTAL SECTION

II-1. Materials

Human eNOS was expressed in baculovirus-SF9 cells and purified as previously described [1, 2]. For this study, eNOS protein was prepared with concentration of 6 mg/ml in the buffer solution including 25 mM Tris-HCl, 100 mM NaCl, 2 mM EGTA and 10% glycerol.

II-2. SAXS measurements

The SAXS measurements were performed at NSRRC on beamline BL23A with 14 keV X-ray beam and Mar CCD detector [3]. The sample-to-detector distance and the absolute intensity were calibrated by using silver behenate and DI water, respectively. The thickness of sample cell was 3 mm in this experiment. The scattering profile, plotted as the scattering intensity (I) versus the scattering vector q , was obtained after corrections for the solvent background, sample transmission, empty cell transmission, and the detector sensitivity.

III. RESULT AND DISCUSSION

Fig. 1 shows the SAXS profile of human eNOS protein in solution with concentration of 6 mg/ml . The scattering curve approaches the Guinier's region at low- q region ($q \leq 0.014 \text{ \AA}^{-1}$), which suggests that the global size of this protein can be extracted from the scattering data. The radius of gyration (R_g) obtained by the Guinier's plot using following equation,

$$I(q) = I_0 \exp\left(-\frac{R_g^2}{3}q^2\right), \quad (1)$$

gives the R_g value to be $6.7 \pm 1.56 \text{ nm}$ (Fig. 2).

The pair-correlation function analysis of the scattering intensity profile is performed through indirect Fourier transform calculated by using GNOM [4, 5]. The R_g can be also calculated from pair-correlation function using the equation, viz [4].

$$R_g^2 = \frac{\int_0^D P(r)r^2 dr}{2 \int_0^D P(r) dr}, \quad P(r) = 0 \text{ for } r \geq D. \quad (2)$$

The results are shown in Fig. 3. The R_g value calculated from the equation (2) is 6.84 nm which is close to that calculated from Guinier's approximation. It also shows the

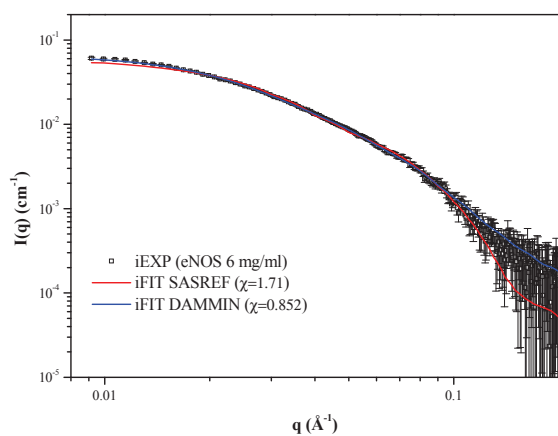


FIG. 1: The SAXS profile of human eNOS protein in solution along with the fitting curves of DAMMIN [6] and SASREF [7].

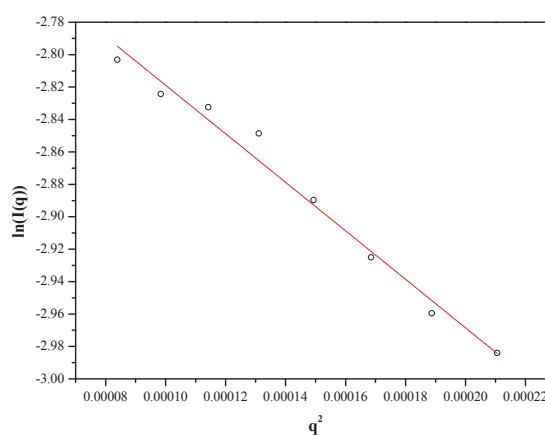


FIG. 2: The Guinier's plot of SAXS profile of human eNOS protein along with linear fitting curve.

maxima size is ca. 22 nm, i.e. 3.21 times higher than the R_g value. This suggests again that the proteins present an extended conformation in solution.

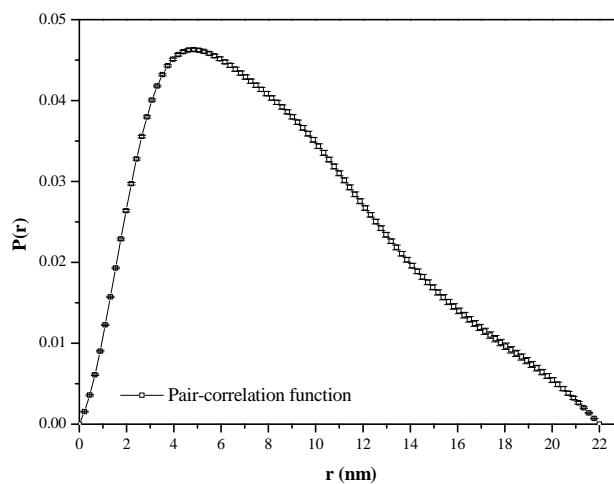
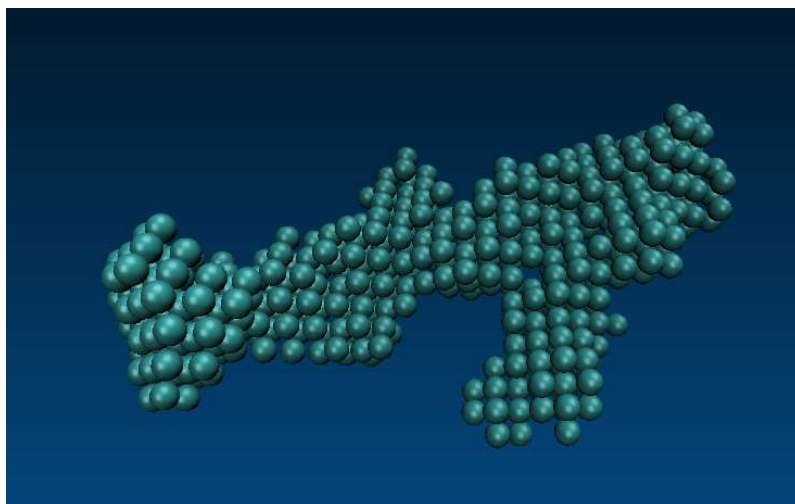


FIG. 3: The pair-correlation function of human eNOS protein in solution calculated by using GNOM [5].

To visualize the envelope structure of the NOS protein, the model fitting of the SAXS profile by DAMMIN using dummy atoms was carried out [6]. The fitted scattering

profile of envelope structure is shown as the solid curve in Fig. 1. It shows good fitting to the experimental scattering profile with the fitting performance of $\chi = 0.852$. The envelope structure of dummy atoms generated by DAMMIN is shown in Fig. 4 (a). The real-space structure was reconstructed by using rigid-body calculation with two known crystal structures of nNOS reductase (1TLL) and eNOS oxygenase (3EAH) to show more realistic structure of eNOS dimer in solution. The SASREF program adjusted the relative orientation and position of individual crystals to fit the experimental SAXS profile of eNOS solution [7]. The final result was illustrated in Fig.4 (b). It can be observed that eNOS formed the dimer structure with the closed contact of their oxygenase domains. This calculated structure was similar with the dimer model proposed in several reports [8, 9]. It

(a)



(b)

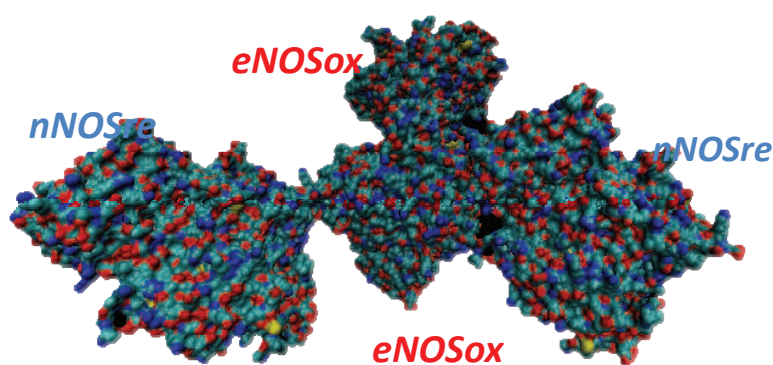


FIG. 4: The real-space structure of (a) dummy atoms generated by DAMMIN with best fit of experimental scattering profile; (b) eNOS dimer calculated by using SASREF with the crystal structures of nNOSre (1TLL) and eNOSox (3EAH).

is believed that human eNOS proteins in solution without the presence of CaM/Ca²⁺ form the homodimers. The flexible linker between oxygenase and reductase domains would be too small to be visualized in the envelope structure.

IV. CONCLUSIONS

The SAXS study of eNOS proteins shows an envelope structure with extended conformation. The radius of gyration and the maxima size were 6.84 nm and 22 nm in solution state, respectively. Homodimer form of eNOS in solution reconstructed by using two crystals shows two oxygenase domains are in close contact. The further studies on eNOS will focus on the dynamics of eNOS in the presence of CaM/Ca²⁺ by using time-resolved spectroscopy.

Acknowledgements

We would like to thank Drs. H. Naitow and N. Kunishima of RIKEN SPring-8 Center and Drs. W. H. Chang and J. H. Lin of Academia Sinica for helpful discussions on protein sample preparation and structural characterization.

References

- [1] P. F. Chen, A. L. Tsai, B. Vladimir, *et al.*, J Biol. Chem. **271**, 14631 (1996).
- [2] P. F. Chen and K. K. Wu, Arch. Biochem. Biophys. **486**, 132 (2009).
- [3] U. S. Jeng, J. Appl. Cryst. **43**, 110 (2010).
- [4] O. Glatter, J. Appl. Cryst. **10**, 415 (1977).
- [5] D. I. Svergun, J. Appl. Cryst. **25**, 495 (1992).
- [6] D. I. Svergun, Biophys. J. **76**, 2879 (1999).
- [7] M. V. Petoukhov and D. I. Svergun, Biophys. J. **89**, 1237 (2005).
- [8] K. Panda, S. Ghosh, and D. J. Stuehr, J. Biol. Chem. **276**, 23349 (2001).
- [9] J. Tejero, L. Hannibal, A. Mustovich, *et al.*, J. Biol. Chem. **285**, 27232 (2010).